Chaotic mixing using periodic and aperiodic sequences of mixing protocols in a micromixer

T.G. Kang*,**, M.K. Singh**, T.H. Kwon* and P.D. Anderson**

* Department of Mechanical Engineering, Pohang University of Science and Technology
Pohang, Kyungbuk 790-784, Republic of Korea
** Materials Technology, Eindhoven University of Technology
PO Box 513, 5600 MB Eindhoven, The Netherlands

ABSTRACT

We numerically studied mixing in a barrier embedded micromixer with an emphasis on the effect of periodic and aperiodic sequences of mixing protocols on mixing performance. A mapping method was employed to investigate mixing in various sequences, enabling us to characterize mixing. Several periodic sequences consisting of the four mixing protocols are chosen to investigate the mixing performance depending on the sequence. Chaotic mixing was observed, but with different mixing performances significantly influenced by the sequence and inertia. As for the effect of inertia, the higher the Reynolds number the larger the rotational motion of the fluid leading to faster mixing. We found that a sequence showing the best mixing performance at a certain Reynolds number is not always superior to other sequences in a different Reynolds number regime. A properly chosen aperiodic sequence results in better mixing than periodic sequences.

Keywords: micromixer, mapping method, mixing protocol, aperiodic sequence

1 INTRODUCTION

We investigated in-depth mixing characteristics of a barrier embedded micromixer (BEM) influenced by periodic and aperiodic sequences of mixing protocols for varying Reynolds numbers. We choose four mixing protocols with specific cross sectional flow portraits created by grooves and the position of a barrier. We obtain periodic velocity fields by solving the incompressible steady Navier-Stokes equations for the protocols and create four mapping matrices for the Reynolds number investigated here. Once a mapping matrix for a mixing protocol is created, the mapping matrix is used to analyze mixing in a sequence consisting of a combination of the four protocols. We investigate mixing in both periodic and aperiodic sequences. The mixing characteristics depending on sequences of the four mixing protocols and inertia will be discussed in detail, showing the progress of mixing both quantitatively and qualitatively using a mapping method and a measure of mixing based on the intensity of segregation.

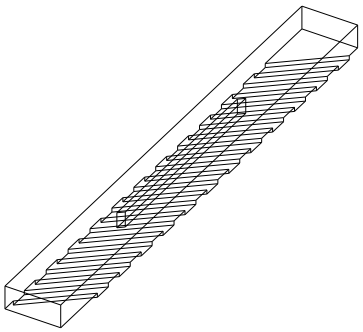

Figure 1: A typical periodic unit of a barrier embedded mixer (BEM).

2 PROBLEM DEFINITION

2.1 Mixing protocols

Figure 1 shows one periodic unit of the BEM with a barrier on the top surface of a rectangular channel and 12 grooves on the bottom. This channel design yields two co-rotating flows with one hyperbolic point and two elliptic points in the section with a barrier and a rotating flow with an elliptic point in the other region without a barrier [1,2]. The four mixing protocols depicted in fig. 2 are designed in such a way that they have particular flow portraits, which are inspired by two-dimensional lid-driven cavity flows as illustrated in fig. 3. The four sets of streamlines shown in fig. 3 represent the overall cross sectional flow characteristics of the four protocols, respectively.

2.2 Governing equations

The periodic velocity field is obtained by solving the steady incompressible Navier-Stokes equations represented by

$$\rho \boldsymbol{u} \cdot \nabla \boldsymbol{u} + \nabla p - \mu \nabla^2 \boldsymbol{u} = \boldsymbol{0} \qquad \text{in } \Omega, \tag{1}$$

$$\nabla \cdot \boldsymbol{u} = 0 \qquad \text{in } \Omega, \tag{2}$$

where ρ denotes the density, $\boldsymbol{u}$ the velocity, p the pressure, and μ the viscosity. The boundary conditions and

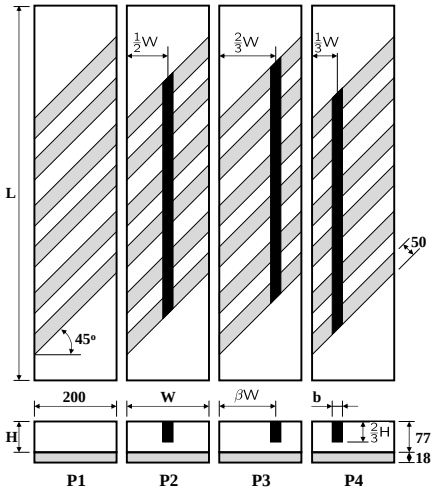

Figure 2: Schematics of the four mixing protocols, P1, P2, P3, and P4, seen from the top and front. The protocol P1 is a rectangular channel with grooves on the bottom surface, while P2, P3, and P4 have a additional barrier on the top surface giving rise to two co-rotating flows. The gray and black areas represent grooves and a barrier, respectively. Length unit: μm.

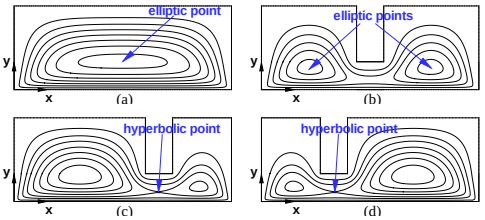

Figure 3: Two-dimensional flow portraits of the four protocols, (a) P1, (b) P2, (c) P3, and (d) P4, in overall sense. The protocols P1 has one elliptic point and the others, P2,P3, and P4, have two elliptic points and one hyperbolic point, but with different lateral positions.

constraint equations are

$$\boldsymbol{u} = \boldsymbol{0} \qquad \text{on } \Gamma_w, \tag{3}$$

$$Q_i = -\int_{\Gamma_i} \boldsymbol{u}\cdot\boldsymbol{n}\mathrm{dS} \qquad \text{on } \Gamma_i, \tag{4}$$

$$\boldsymbol{u}_i = \boldsymbol{u}_o \qquad \text{on } \Gamma_i \text{ and } \Gamma_o, \tag{5}$$

where Q_i is the imposed flow rate through the inlet, $\boldsymbol{n}$ the outward unit normal vector at the boundary Γ_i, $\boldsymbol{u}_i$ the velocity at the inlet node, and $\boldsymbol{u}_o$ the velocity at the outlet node. In the above equations (Eqs. (1)-(5)) Ω, Γ_w, Γ_i, and Γ_o denote the entire bounded domain, the solid wall boundaries, the inlet boundary, and the outlet boundary, respectively. The Reynolds number is given by $\mathrm{Re} = \rho D_h U_a/\mu$, where D_h is the hydraulic diameter of the rectangular channel and U_a the average velocity at the inlet.

3 MAPPING METHOD

3.1 Mapping method

A mapping method [3] was employed to investigate mixing in various sequences to qualitatively observe the progress of mixing and also to quantify both the rate and the final state of mixing. The mapping method describes the transport of materials (represented by the concentration function varying from 0 to 1) from one cross section to the next in channel flows. A matrix called the mapping matrix stores information about the distribution of fluid from one cross-section to the next (spatially periodic flows), which arises due to a specified flow. Given periodic velocity fields as a solution of the Navier-Stokes equations for the four protocols at a fixed Reynolds number, mapping matrices for the protocols are computed and are used to analyze mixing in a sequence consisting of a combination of the protocols. The evolution of a concentration vector after n periods $\boldsymbol{C}^n$ is computed in sequence as follows:

$$\boldsymbol{C}^{i+1} = \boldsymbol{\Phi}\boldsymbol{C}^i, \text{ hence } \boldsymbol{C}^n = (\underbrace{\boldsymbol{\Phi}(\boldsymbol{\Phi}(\ldots(\boldsymbol{\Phi}\boldsymbol{C}^0)))}_{n \text{ times}}). \tag{6}$$

where $\boldsymbol{\Phi}$ is the mapping matrix. Thus, the mapping matrix is calculated only once and is utilized a number of times to study the evolution of concentration in the flow field. For validation of the mapping method and other details, we refer to [3-5] and references therein.

3.2 Measure of mixing

We quantify the progress of mixing by the intensity of segregation I_d of the concentration c_i at N discrete points. The intensity of segregation is defined as follows:

$$I_d = \frac{1}{\bar{c}(1-\bar{c})}\frac{1}{N}\sum_{i=1}^{N}(c_i - \bar{c})^2, \tag{7}$$

where $\bar{c}$ is the average concentration. The intensity of segregation (I_d) is a measure of the deviation of the local concentration from the ideal situation (perfectly mixed), which represents a homogeneous state of the mixture. In the mixing analysis, we define a mixing quality Q, defined as $Q = 1 - I_d$, as a measure of mixing. In a perfectly mixed system, $Q = 1$, while in a completely unmixed system, $Q = 0$.

4 RESULTS

4.1 Periodic sequences

We begin with periodic sequences composed of a repeating unit, which may be one mixing protocol or a set of protocols. We propose five periodic sequences as

NSTI-Nanotech 2007, www.nsti.org, ISBN 1420061844 Vol. 3, 2007

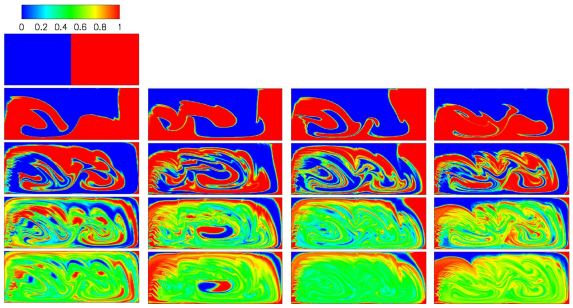

(a) P12 (b) P34 (c) P32 (d) P42

Figure 4: Evolution of mixing patterns at Re=0.01. The color contours represent the concentration at several down-channel positions z=4, 10, 20, and $30L$, for the four periodic sequences. The concentration at z=0 is plotted at the top of the column.

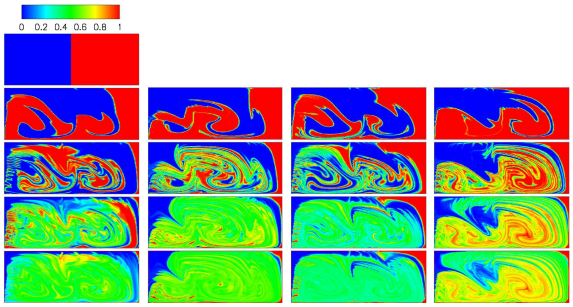

(a) P12 (b) P34 (c) P32 (d) P42

Figure 5: Evolution of mixing patterns at Re=30. The color contours represent the concentration at several down-channel positions z = 4, 10, 20, and $30L$, for the four periodic sequences.

follows:

$$P11 : \mathbf{111111} \cdots \mathbf{111111}, \quad (8)$$
$$P12 : \mathbf{121212} \cdots \mathbf{121212}, \quad (9)$$
$$P34 : \mathbf{343434} \cdots \mathbf{343434}, \quad (10)$$
$$P32 : \mathbf{323232} \cdots \mathbf{323232}, \quad (11)$$
$$P42 : \mathbf{424242} \cdots \mathbf{424242}, \quad (12)$$

where a boldface number **1** represents the protocol P1, **2** the protocol P2, and so on (see fig. 2). The first sequence $P11$ is just a channel with slanted grooves without any mechanism to induce chaotic advection, while the others are chaotic micromixers which will be discussed shortly. We use $P12$ as a reference state to compare relative mixing performances of proposed sequences.

First introduced are the results of mixing at Re = 0.01 where flow is mainly governed by the viscous force only. Figure 4 shows the evolution of mixing patterns for the four periodic sequences. The picture on the top of fig. 4(a) depicts the initial unmixed state at the inlet, z = 0, and the following four pictures show the progress of mixing along down-channel positions, z = 4, 10, 20, and $30L$. At the inlet, the concentration at nodal points c_i is either 0 or 1 depending on the species of the fluid. Assuming two fluids are introduced through a T-type inlet channel, the concentration c_i equals 0 in the left half and 1 in the right half (see the first picture of fig. 4(a)). At the interface of two fluids, the value of c_i is 0.5 representing a completely mixed state. Mixing in the protocol $P12$ is almost chaotic except for several unmixed islands. As for $P34$, we see a unmixed island at the center, which indicates the existence of a KAM (Kolmogorov-Arnold-Moser) boundary at that location. The other two sequences, $P32$ and $P42$, are globally chaotic except the rim of the rectangular channel, better than $P12$ and $P34$ from the viewpoint of the existence of unmixed islands. The mixing performance of $P32$ seems to be the best among the five sequences in the creeping flow regime using the mixing quality Q as a mixing measure.

We also investigate the effect of inertia on the flow and mixing characteristics for the same periodic sequences. Here, the effect of inertia on the mixing performance will be studied for the flow with Re=0.01, and 30. From the concentration plots showing mixing patterns in fig. 5, we are able to observe the increased rotational motion of fluids with higher inertia compared with fig. 4. As the Reynolds number increases, the unmixed islands shown in figs. 4(a) and 4(b) for the two sequences, $P12$ and $P34$, are completely disappeared indeed as shown in figs. 5(a) and 5(b), demonstrating a positive influence of inertia on mixing in the two sequences.

4.2 Aperiodic sequences

It is known that aperiodic flows generate widespread chaos even under conditions where periodic flows generate minimal or no chaos [6]. Motivated by this fact, we conduct simulations in aperiodic sequences attempting to find out a sequence of protocols which results in better mixing compared with periodic sequences.

We create aperiodic sequences at Re=0.01 and 30 such that at a given mixing protocol the next protocol is chosen to give the best mixing state among the four candidates. Two aperiodic sequences chosen by the above-mentioned scheme at Re=0.01 are

$$AP1 : \mathbf{32323\ 23233\ 23323\ 31232\ 22233\ 31222}, \quad (13)$$
$$AP2 : \mathbf{42243\ 22333\ 33333\ 42222\ 43331\ 42231}, \quad (14)$$

where an aperiodic sequence $AP1$ start with $P3$ and $AP2$ with $P4$. At Re=30, two other aperiodic sequences (starting from **3** and **4**) generated in the same way are given by

$$AP3 : \mathbf{32323\ 42222\ 22222\ 24222\ 21222\ 12211}, \quad (15)$$
$$AP4 : \mathbf{43323\ 42222\ 22222\ 22222\ 21412\ 12111}. \quad (16)$$

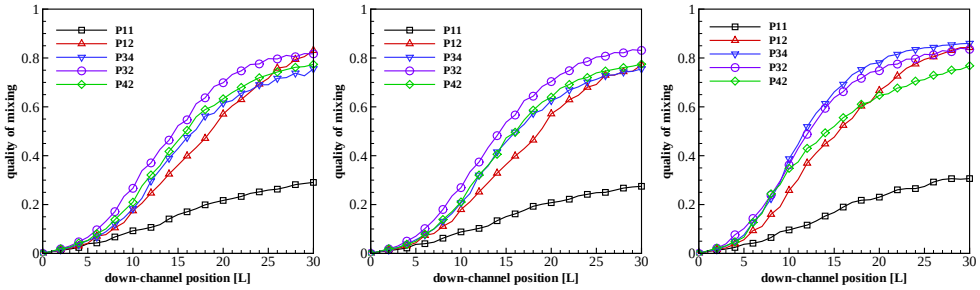

(a) Re=0.01 (b) Re=5 (c) Re=30

Figure 6: Evolution of mixing quality Q of five periodic sequences at three different Reynolds numbers. The abscissa is a down-channel position z scaled by the length of one mixing protocol L.

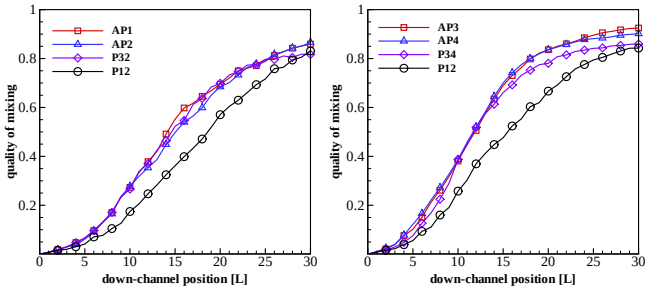

(a) Re=0.01 (b) Re=30

Figure 7: Evolution of mixing quality Q of two aperiodic sequences at two Reynolds numbers. The mixing quality Q of two periodic sequences also plotted for comparison. The abscissa is a down-channel position z scaled by the length of one mixing protocol L.

The evolution of mixing quality Q with the down-channel position z is plotted in fig. 7 together with the results from two periodic sequences, P12 as a reference and another sequence showing the best performance at each Reynolds number. The two aperiodic sequences found at two Reynolds numbers show better mixing performance (measured by Q) than the reference sequence (P12) and the best sequence at each Reynolds number, implying the existence of an optimum sequence.

5 CONCLUSIONS

We investigated the effect of mixing protocols constituting periodic and aperiodic sequences in a barrier embedded micromixer using a mapping method. Given functional modules (called mixing protocols) with specific flow portraits, mixing in several periodic and aperiodic sequences composed of those protocols are analyzed for the varying Reynolds number. Both mixing rate and final mixing state of the chosen sequences show noticeable differences compared with the results from the original BEM. As for the effect of inertia, the higher the Reynolds number the faster and the more uniform mixing (within the limit of micromixers investigated in the present study). A sequence showing the best performance at a low Reynolds number does not always guarantee the best performance at other Reynolds number. A properly chosen aperiodic sequence indeed shows better mixing than mixers consisting of periodic sequences.

REFERENCES

[1] D.S. Kim, S.W. Lee, T.H. Kwon, and S.S. Lee, J. Micromech. Microeng., 14, 798–805, 2004.

[2] T.G. Kang and T.H. Kwon, J. Micromech. Microeng., 14(7), 891–899, 2004.

[3] O.S. Galaktionov, P.D. Anderson, G.W.M. Peters and H.E.H. Meijer, Int. J. Numer. Methods Fluids, 40(1-2), 189–196, 2002.

[4] P.G.M. Kruijt, O.S. Galaktionov, G.W.M. Peters and H.E.H. Meijer, Int. Polym. Process, XVI(2), 161–171, 2001.

[5] M.K. Singh, P.D. Anderson and H.E.H. Meijer, Lab. Chip., submitted.

[6] M. Liu, F.J. Muzzio and R.L. Peskin, Chaos, Solitons & Fractals, 4(6),869–893, 1994.